

Original Research

Inhibition of TRAP1 Accelerates the DNA Damage Response, Activation of the Heat Shock Response and Metabolic Reprogramming in Colon Cancer Cells

Nobel Bhasin^{1,†}, Prerna Dabral^{1,†}, Lakmini Senavirathna², Sheng Pan², Ru Chen^{1,*}¹Section of Gastroenterology and Hepatology, Department of Medicine, Baylor College of Medicine, Houston, TX 77030, USA²The Brown Foundation Institute of Molecular Medicine, University of Texas at Houston Health Science Center, Houston, TX 77030, USA*Correspondence: ru.chen@bcm.edu (Ru Chen)

Academic Editor: Alfonso Urbanucci

Submitted: 28 June 2023 Revised: 29 July 2023 Accepted: 24 August 2023 Published: 26 September 2023

Abstract

Background: Colorectal cancer (CRC) is one of the major causes of cancer-related mortality worldwide. The tumor microenvironment plays a significant role in CRC development, progression and metastasis. Oxidative stress in the colon is a major etiological factor impacting tumor progression. Tumor necrosis factor receptor-associated protein 1 (TRAP1) is a mitochondrial member of the heat shock protein 90 (HSP90) family that is involved in modulating apoptosis in colon cancer cells under oxidative stress. We undertook this study to provide mechanistic insight into the role of TRAP1 under oxidative stress in colon cells. **Methods:** We first assessed the The Cancer Genome Atlas (TCGA) CRC gene expression dataset to evaluate the expression of TRAP1 and its association with oxidative stress and disease progression. We then treated colon HCT116 cells with hydrogen peroxide to induce oxidative stress and with the TRAP1 inhibitor gamitrinib-triphenylphosphonium (GTPP) to inhibit TRAP1. We examined the cellular proteomic landscape using liquid chromatography tandem mass spectrometry (LC-MS/MS) in this context compared to controls. We further examined the impact of treatment on DNA damage and cell survival. **Results:** TRAP1 expression under oxidative stress is associated with the disease outcomes of colorectal cancer. TRAP1 inhibition under oxidative stress induced metabolic reprogramming and heat shock factor 1 (HSF1)-dependent transactivation. In addition, we also observed enhanced induction of DNA damage and cell death in the cells under oxidative stress and TRAP1 inhibition in comparison to single treatments and the nontreatment control. **Conclusions:** These findings provide new insights into TRAP1-driven metabolic reprogramming in response to oxidative stress.

Keywords: TRAP1; colon cancer; proteomics; oxidative stress

1. Introduction

Colorectal cancer (CRC) is a multifactorial disease. In addition to the major driver genes (such as *P53*, *KRAS*, and *BRAF*) that lead to molecular pathways for the pathogenesis of CRC, several other important molecular phenomena are altered in neoplastic pathology [1]. The generation of oxidative stress is one such phenomenon that plays a paradoxical role. While increased oxidative stress may induce genetic instability leading to neoplastic transformation, excessive production of reactive oxygen species (ROS) makes the tumor sensitive to ROS insults.

Under normal conditions, ROS regulate many signal transduction pathways involved in cell proliferation and survival. Under the conditions of oxidative stress, the antioxidant capacity of the cells may be overwhelmed. This manifests in redox adaptation, where cells undergo a metabolic shift to enhance proliferation and oncogenic signaling [2–5]. Nevertheless, excessive reliance on elevated production of ROS makes tumor cells increasingly vulnerable to further ROS insults, and such sustained redox perturbation could be instrumental in preferentially eliminating them [2–5]. ROS induce DNA damage and genomic in-

stability by introducing single- and double-stranded DNA breaks and the formation of apurinic/apyrimidinic lesions [6]. Under high-oxidative stress conditions, such as colitis-associated CRC, colon cancer cells rely on antioxidant molecules for survival. Therefore, genes that mitigate oxidative stress play a protective role in the tumor microenvironment [7,8].

Tumor necrosis factor receptor-associated protein 1 (TRAP1) is a mitochondrial chaperone that belongs to the heat shock protein 90 (HSP90) family of chaperones [9]. The role of TRAP1 in cancer has been explored across different malignancies and microenvironments [10]. Its expression is upregulated in several malignancies, including colon breast cancer, prostate cancer, glioblastoma and lung cancer [9,11–13]. Studies have shown that TRAP1 plays an essential role in neoplastic transformation and precursor lesions of colitis-associated CRC [14,15]. TRAP1 expression has also been associated with metastasis and correlated with drug resistance [11,16]. High expression of TRAP1 in colon cancer is associated with lymph node metastasis and poor overall survival [11,17]. It is evident through multiple studies that TRAP1 plays a context- and cancer type-dependent role [11,18,19]. A recent report from our lab



further demonstrated differential modulation of oxidative stress by TRAP1 in colon cancer cell lines [20]. We undertook this study to examine the resistance to cell death modulated by TRAP1 under oxidative stress in colon cancer.

2. Materials and Methods

2.1 TCGA Data Inquiry

The colon cancer subset of The Cancer Genome Atlas (TCGA) PanCancer Atlas data on CRC was examined in patients with +1 and -1 standard deviation (SD) of mean expression of NFKB1 and TRAP1 [21]. CBioportal was used to examine the clinical profile of the patients [22,23].

2.2 Cells, Reagents and Treatment

The colon cancer cell line HCT116 was a gift from the laboratory of Dr. Noah Shroyer at Baylor College of Medicine, which was originally purchased from the American Type Culture Collection (Manassas, VA, USA) under the catalog number CCL-247 without Mycoplasma contamination. The cell line was authenticated by the American Type Culture Collection (ATCC®), using seventeen short tandem repeat (STR) loci plus the gender determining locus, Amelogenin, with the commercially available PowerPlex® 18D Kit from Promega (Manassas, VA, USA). The cells were cultured in DMEM, 2 mM L-glutamine, 10% (v/v) fetal bovine serum (FBS), 100 U/mL penicillin, and 100 µg/mL streptomycin in a 37 °C incubator at 5% CO₂. The cell culture reagents were purchased from Fisher Scientific (Hampton, NH, USA). The TRAP1 inhibitor gamitrinib-triphenylphosphonium (GTPP) was purchased from MedChem Express (HY-102007A) (Monmouth Junction, NJ, USA). Phospho-Histone H2AX (γH2AX), Thioredoxin reductases 2 (TRXR2/TXNRD2) and β-actin antibodies were purchased from Cell Signaling Technology (Danvers, MA, USA). For all experiments, HCT116 cells were treated with 10 µM H₂O₂, 5 µM GTPP or both 10 µM H₂O₂ and 5 µM GTPP with control samples as untreated cells for a period of 24 hours, unless otherwise specified.

2.3 Trypan Blue Exclusion Assay

Cell death was estimated using the Trypan Blue exclusion assay. Briefly, HCT116 cells were seeded in 6-well plates and subjected to different treatment conditions for 24 hours. Subsequently, an aliquot of the cells was mixed with 0.2% trypan blue at a ratio of 1:1 by volume. The cell suspension was counted using a hemocytometer chamber under a light microscope.

2.4 Cell Viability Assay

The viability of HCT116 cells was examined using the Cell Proliferation assay (MTT) with reagents purchased from Roche Life Science as per the manufacturer's guidelines (Basel, Switzerland). A total of 5000 HCT116 cells were plated in the growth media described above. Cells

were then treated with a combination of 10 µM H₂O₂ and 0–7 µM GTPP for 24 hours. The experiment was repeated 3 times. Cell viability relative to control was plotted using GraphPad Prism from GraphPad Software (version 8, Boston, MA, USA) [24].

2.5 Western Blotting

Cells were lysed in Mammalian Protein Extraction Reagent (MPER) buffer with 1× Halt Protease inhibitor cocktail from Fisher Scientific (Hampton, NH, USA). The protein lysate was resolved using a 4–15% SDS–PAGE gel from Bio-Rad Laboratories (Hercules, CA, USA) and transferred onto a 0.2 µM polyvinylidene fluoride (PVDF) membrane using the iBlot2 dry blotting system from Fisher Scientific (Hampton, NH, USA) following the manufacturer's instructions. The membranes were incubated with primary antibodies followed by secondary horseradish peroxidase (HRP)-tagged antibodies and imaged on Gel-Doc EX images from Bio-Rad Laboratories (Hercules, CA, USA).

2.6 Immunofluorescence Assay

Approximately 1×10^5 cells (under different treatment conditions) were plated on coverslips and washed with 1× PBS three times. The cells were fixed with 4% formaldehyde for 10 minutes at room temperature and washed with 1× PBS three times. The cells were permeabilized with 0.5% Triton X-100 in PBS at room temperature for 5 minutes and washed with 1× PBS three times. The cells were then blocked with 5% normal goat serum in 1× PBS for 1 hour. After washing with PBS, the cells were incubated with the primary antibody (γH2AX, 1:100) overnight at 4 °C. The next day, following three washes with 1× PBS, the cells were incubated with Alexa Fluor 488-conjugated goat anti-rabbit IgG secondary antibody at a concentration of 1:1000 for 1 hour at room temperature in the dark. The cells were washed with 1× PBS three times and stained with DAPI from Fisher Scientific (Hampton, NH, USA) at a concentration of 1:1000 at room temperature for 3 minutes. After the final three washes with 1× PBS, the coverslips were mounted on slides using ProLong™ Gold Antifade Mountant from Fisher Scientific (Hampton, NH, USA). The slides were analyzed using a Nikon florescent microscope, and quantification of foci was performed using ImageJ (version 2.14, <https://imagej.net/software/fiji/>) [25].

2.7 Proteomic Sample Preparation

The cells were lysed in MPER buffer (+1X Halt Protease inhibitor cocktail), and the cell debris was pelleted by centrifugation at 14,000 ×g for 10 minutes at 4 °C. For each sample, the supernatant was collected, and 100 µg of protein was processed for proteomic analysis as previously described [26]. Briefly, the protein lysates were reduced with 10 mM Dithiothreitol (DTT) at 50 °C for 1 hour, followed by alkylation using 25 mM iodoacetamide at room temper-

ature for 30 minutes in the dark. The proteins were precipitated using a 1/4th volume of 100% (w/v) trichloroacetic acid (TCA) for 30 minutes on ice. The samples were centrifuged at $14,000 \times g$ for 10 minutes at 4°C . The pellets were rinsed twice with ice-cold acetone followed by centrifugation at $14,000 \times g$ for 10 minutes. The protein pellets were air dried and resuspended in 50 mM ammonium bicarbonate. Trypsin was added at a 1:30 ratio in two steps with a 2-hour incubation in between with vortexing every 30 minutes. The samples were finally incubated overnight at 37°C (approximately 18 hours). The samples were centrifuged briefly, and the peptide concentration was measured using the BCA Gold assay. The samples were dried completely in Savant™ SpeedVac™ (ThermoFisher Scientific, Waltham, MA, USA) and resuspended at 1 mg/mL in 0.1% formic acid for MS analysis.

2.8 LC MS/MS Analysis

One microgram of each digested sample was analyzed with a Q Exactive™ HF-X Orbitrap™ mass spectrometer (ThermoFisher Scientific, Waltham, MA, USA) interfaced with an UltiMate 3000 HPLC (ThermoFisher Scientific) as described previously [27]. The sample was first loaded into a 5-mm trap column packed with $5\ \mu\text{M}/100\ \text{\AA}$ C18 material (Thermo Fisher Scientific) using 98% buffer A (0.1% formic acid in water) and 2% buffer B (0.1% formic acid in acetonitrile) at a flow rate of $3\ \mu\text{L}/\text{min}$. The peptides were separated in a 25 cm analytical column packed with $5\ \mu\text{M}/18\ \text{\AA}$ C18 material using a 90-minute linear gradient ramping from 2% to 35% buffer B versus buffer A at a flow rate of $0.35\ \mu\text{L}/\text{min}$. Mass spectrometric analysis was performed using data-dependent acquisition (DDA) mode. The survey scan was performed with 60K resolution from 400 to 1600 m/z with an automatic gain control (AGC) target of $3e6$ and a max injection time of 50 msec. Monoisotopic masses were then selected for further fragmentation for the 25 most abundant precursor ions with 2 to 4 plus charges. Precursor ions were isolated using the quadrupole with an isolation window of 1.6 m/z . Higher energy collisional dissociation (HCD) was applied with a normalized collision energy of 28%. Tandem mass spectrometry (MS/MS) scans were carried out with a resolution of 7500. The AGC target for MS/MS was set to $5e5$, and the maximum injection time was limited to 22 msec.

2.9 Mass Spectrometric Data Analysis

The MS data were searched against the UniProt human protein database for peptide/protein identification using the Comet algorithm embedded in the Trans-Proteomic Pipeline [28,29]. Carbamidomethylation of cysteine was set as a fixed modification, and oxidation of methionine and deamidation of asparagine were set as variable modifications. The peptide assignment was validated with PeptideProphet, and a probability score ≥ 0.9 in correspondence with an error rate of 0.01 was applied to filter the peptides.

Skyline software (version 21.1.0.146, <https://skyline.ms/>) was used for quantitative analysis of the DDA data [30,31]. The spectral library-based platform described in previous studies was used for quantitative analysis [26,32,33]. The composite spectral library was built using all of the DDA data collected from the samples analyzed. Quantification was performed at the MS1 level using the sum of the first 3 monoisotopic peaks. The abundance of each peptide was normalized to the total ion current (TIC) and presented as ion per million (IPM) using the following formula: Normalized Intensity (IPM) = Peptide Intensity/TIC $\times 1000000$. Protein quantification was achieved by summation of the normalized intensities of the corresponding peptides.

2.10 Statistical and Enrichment Analysis

The log-rank test was used to compare the survival of colon cancer patients in the TCGA dataset. A p value of <0.05 was considered significant. To compare the occurrence of new neoplasms post initial therapy, a chi-squared test was performed, and a p value < 0.05 was considered significant. Differential expression analysis of TCGA data was performed on cBioportal, keeping a threshold of 10% false discovery rate (FDR) [23]. Gene set enrichment analysis (GSEA) was performed using the WebGestalt online tool [34,35]. An FDR cutoff of 5% was applied to GSEA.

The protein ratios between the treatment groups and the control group were analyzed by calculating $\log_2\text{FoldChange}$. Differential protein expression was calculated using the limma package in R (version 3.17, <https://www.bioconductor.org/>) [36]. The differentially expressed genes were filtered by an FDR of 0.15. Hierarchical clustering, sample correlation and principal component analysis were performed using the online bioinformatics platform idep.96 [37]. Cluster enrichment was performed using Metascape [38].

3. Results

3.1 TRAP1 Expression Under Oxidative Stress is Associated with Disease Outcomes

To examine the impact of TRAP1 expression on colon cancer, we analyzed the mRNA expression of TRAP1 and its association with progression-free survival and disease-specific survival using TCGA data. First, we used the mRNA expression of NFKB1 to represent the oxidative stress level of a patient. Patients with NFKB1 expression 1 SD higher or lower than the mean value were designated as the patients with high oxidative stress or low oxidative stress, respectively. Accordingly, patients with a TRAP1 expression more than 1 SD higher than the average were classified as high TRAP1, and those below 1 SD were classified as low TRAP1. Under low oxidative stress conditions, patients with either low or high TRAP1 expression did not show a significant difference in either progression-free or disease-specific survival (Fig. 1A,B). Notably, under high oxidative stress conditions, however, the patients with

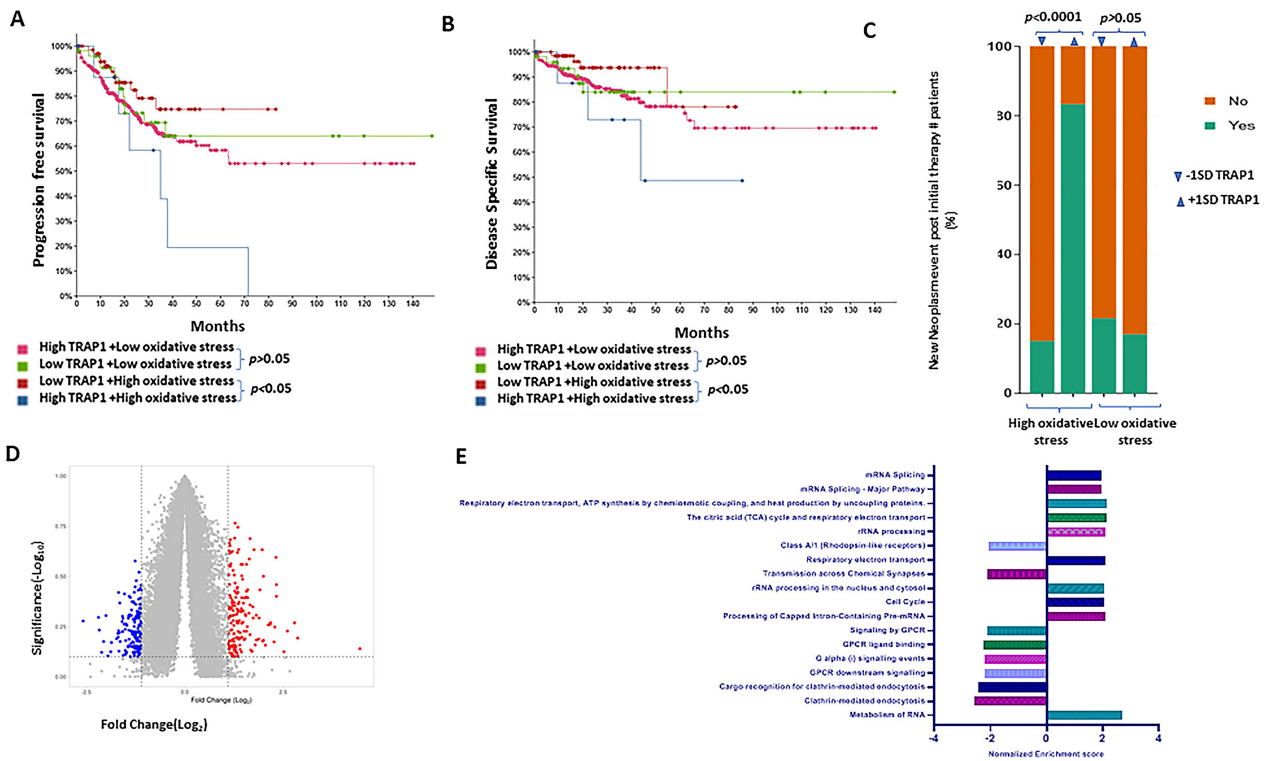


Fig. 1. Tumor necrosis factor receptor-associated protein 1 (TRAP1) expression under oxidative stress is associated with disease outcomes in The Cancer Genome Atlas (TCGA) colorectal cancer data. (A) Progression-free survival. (B) Disease-specific survival in patients with high and low expression of TRAP1 under high and low oxidative stress. (C) Percentage of patients who develop a new neoplasm postinitial therapy. (D) Volcano plot, (E) Gene set enrichment analysis of differentially expressed genes in patients with high and low TRAP1 expression under high oxidative stress (+1 SD NFKB1 expression).

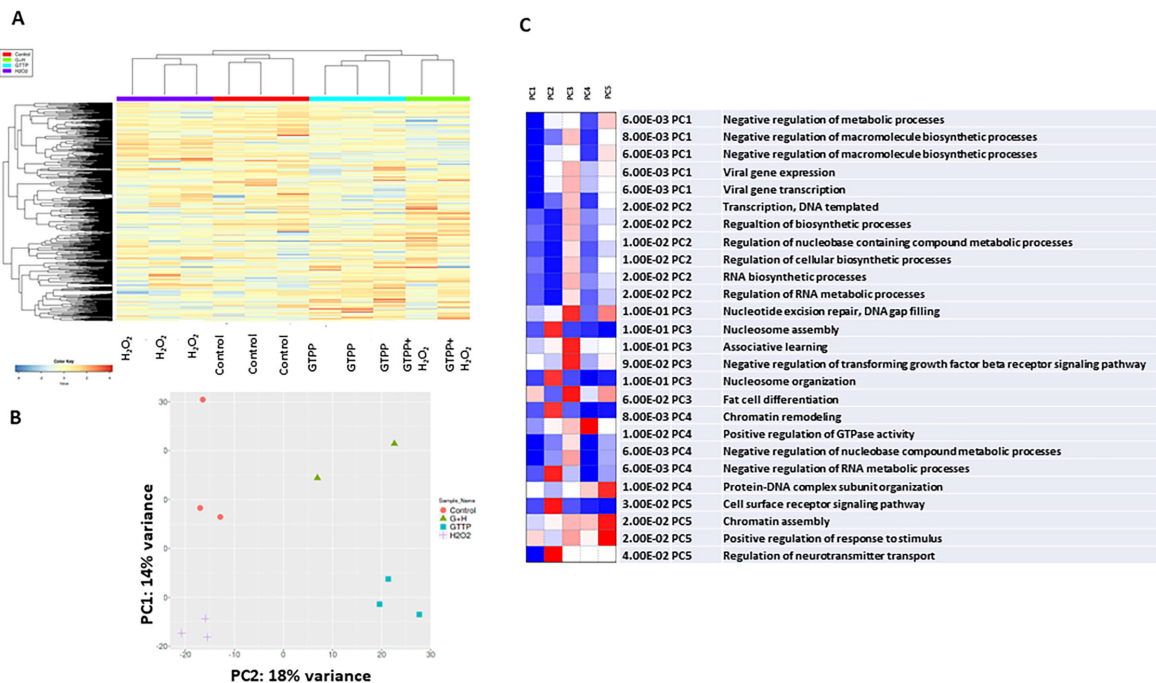


Fig. 2. Proteomic profiling of TRAP1 inhibition in colon cancer cells under oxidative stress. (A) Heatmap showing the Z score of top 1000 most variable proteins. (B) Principal component analysis of proteomic expression in control or after treatment with combination of GTPP+H₂O₂ or H₂O₂ or GTPP alone. (C) Gene ontology of PCs driving the response.

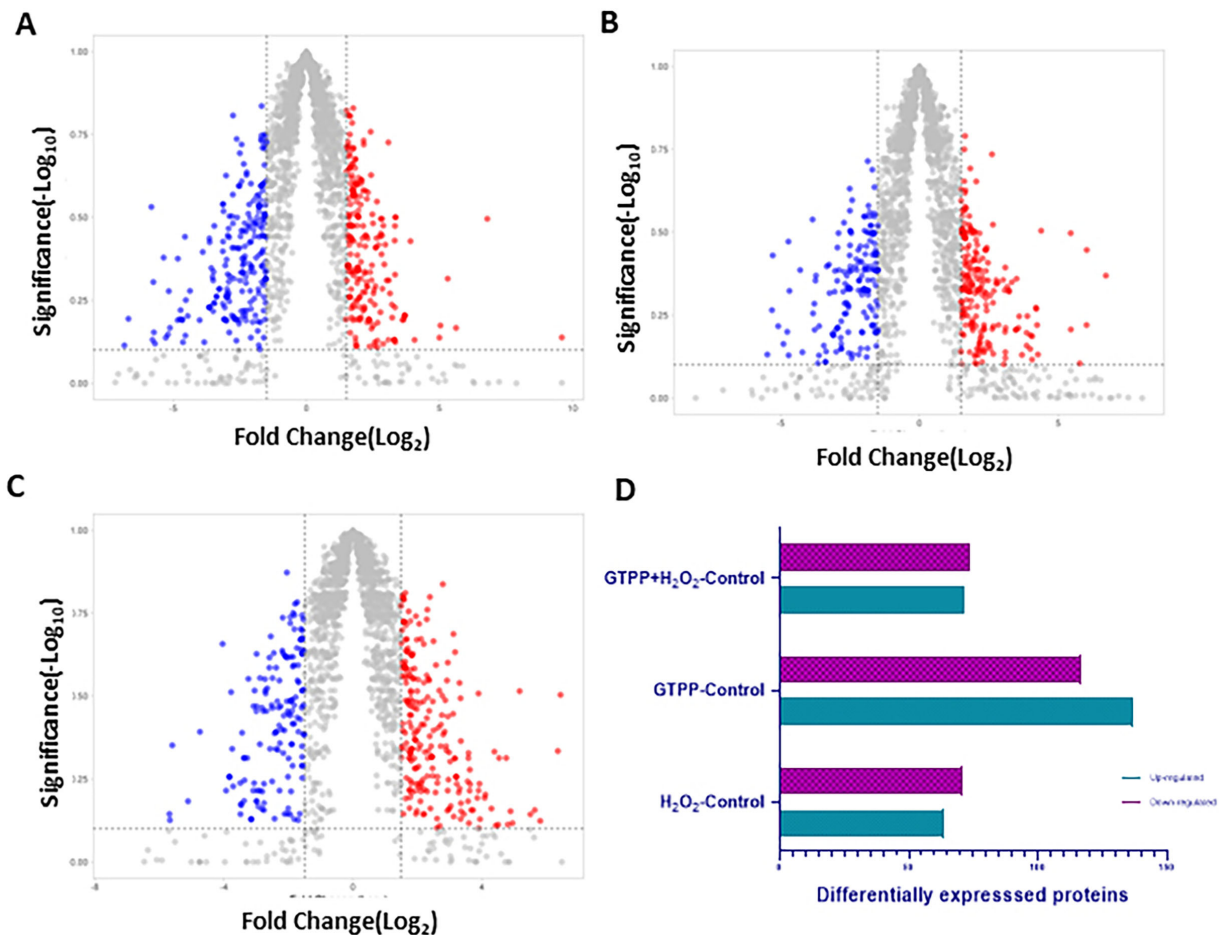


Fig. 3. Differential protein expression after TRAP1 inhibition under oxidative stress in colon cancer cells. (A–C) Volcano plots of protein ratios in comparison to the control group for GTPP+H₂O₂ (A), GTPP (B), and H₂O₂ (C). (D) Differentially upregulated and downregulated proteins with different treatments.

high TRAP1 expression had a significantly shorter survival time for both progression-free and disease-specific survival in comparison to those with low TRAP1 levels ($p < 0.05$, Fig. 1A,B).

Additionally, for patients with high oxidative stress, the group with high TRAP1 expression had a higher risk for developing new neoplasms postinitial therapy than the group with low TRAP1 expression ($p < 0.0001$) (Fig. 1C). In contrast, patients with low oxidative stress showed no significant difference between low and high TRAP1 expression in the risk of developing a new neoplasm post initial therapy (Fig. 1C).

Our analysis of differential mRNA expression between TRAP1 high- and TRAP1 low-expressing tumors under high oxidative stress showed 974 differentially expressed genes, as visualized by the volcano plot in Fig. 1D. GSEA-based query using the Reactome pathway database showed an enrichment of pathways associated with RNA splicing, cellular metabolism, G protein coupled receptor signaling and cell division [35,39] (Fig. 1E). **Supplementary Tables 1,2** summarize the list of differentially ex-

pressed genes and enrichment results, respectively. Altogether, the gene expression analysis of the TCGA CRC dataset suggested that TRAP1 expression was associated with patient survival when the tumors were under high oxidative stress. This prompted us to further explore the implication of TRAP1 for CRC therapeutic benefits in the context of high oxidative stress at the functional level using a proteomic approach.

3.2 Proteomic Landscape of Colon Cancer Cells Under Oxidative Stress and TRAP1 Inhibition

To examine the proteome alterations induced by oxidative stress and/or modulated by TRAP1, colon cancer HCT116 cells were treated with H₂O₂ to mimic oxidative stress in colon cancer, with or without TRAP1 inhibition using GTPP. The H₂O₂ concentration reflecting a state of oxidative stress was used [40]. A cell viability assay with 0–7 μ M GTPP in combination with 10 μ M H₂O₂ was performed to determine the appropriate dose for treatment. The concentration of H₂O₂ was selected based on the H₂O₂ dose response [13]. **Supplementary Fig. 1** shows the dose re-

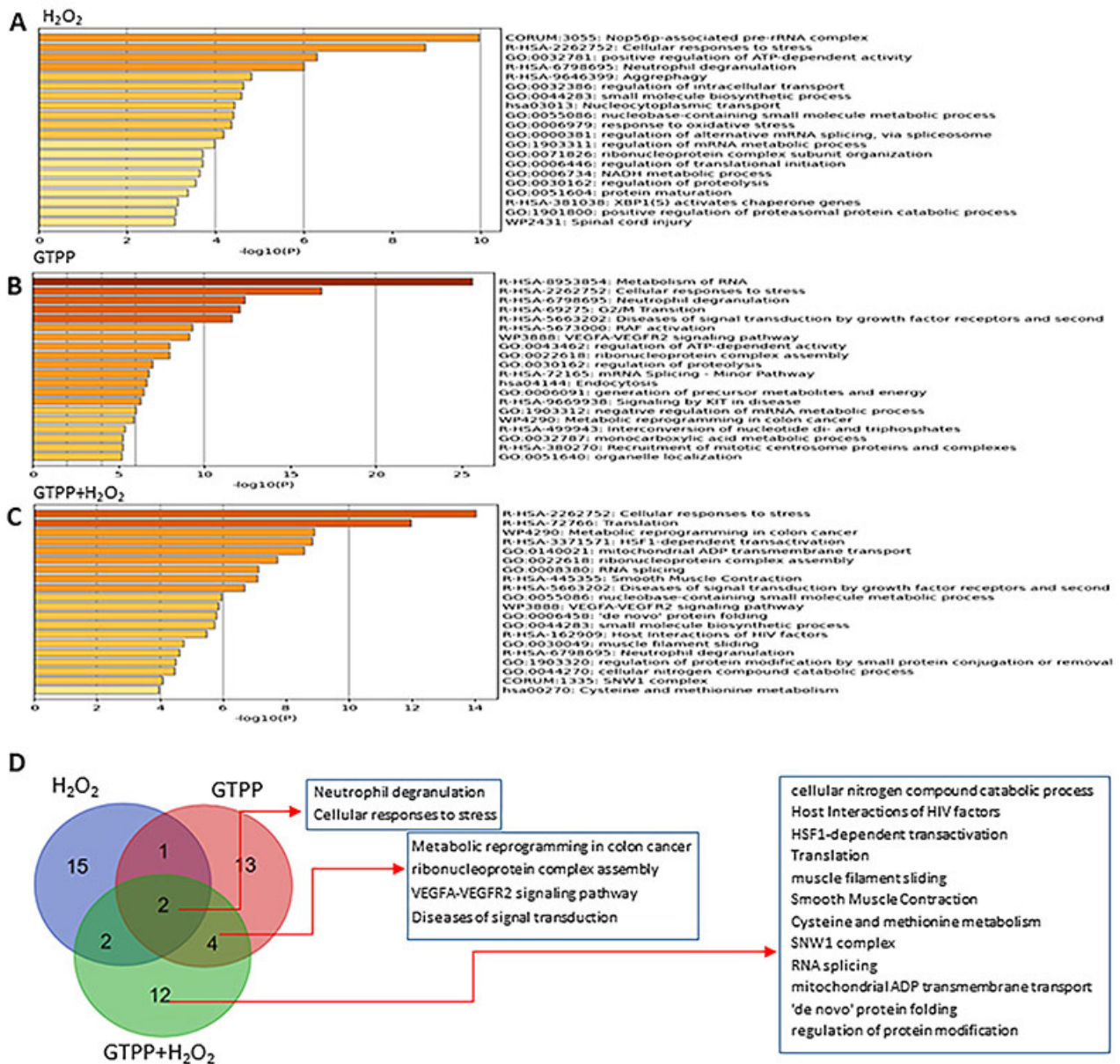


Fig. 4. Functional enrichment of differentially expressed proteins. Enriched clusters were examined in differentially expressed proteins. Comparisons are as follows H₂O₂ vs. Control (A), GTPP vs. Control (B), GTPP+H₂O₂ vs. Control (C). Venn diagram of primary overlapping and exclusive clusters in the three comparisons (D).

sponse curve after 24 hours of treatment. A dose of 5 μ M GTPP in combination with 10 μ M H₂O₂ showed an average of 57.66% cell viability. This dose was selected to treat the cells for proteomic analysis.

Using the spectral library-based platform, a total of 3240 proteins were identified (FDR <0.01) and quantified in these samples. The adjusted *p* value and fold change for each protein in the three treatment groups, including H₂O₂ only, GTPP only and H₂O₂+GTPP, compared to the control group are presented in **Supplementary Table 3**. The top 1000 most variable proteins were visualized as a heatmap of z score across the four groups (Fig. 2A). Samples were clustered together with respect to their treatment groups.

Additionally, samples were further clustered with respect to GTPP or no-GTPP treatments. Principal component analysis (PCA) confirmed the results from hierarchical clustering (Fig. 2B). PCA also demonstrated that GTPP treatment drove 18% of the variance (PC1) in proteomic profiles, followed by H₂O₂ treatment, which drove 14% of the variance (PC2) (Fig. 2B). Gene ontology enrichment of the pathways in each principal component showed enriched pathways related to negative regulation of metabolic process and negative regulation of biosynthetic process in PC1 (Fig. 2C). PC2 showed an enrichment of DNA-templated RNA transcription and regulation of biosynthetic processes (Fig. 2C).

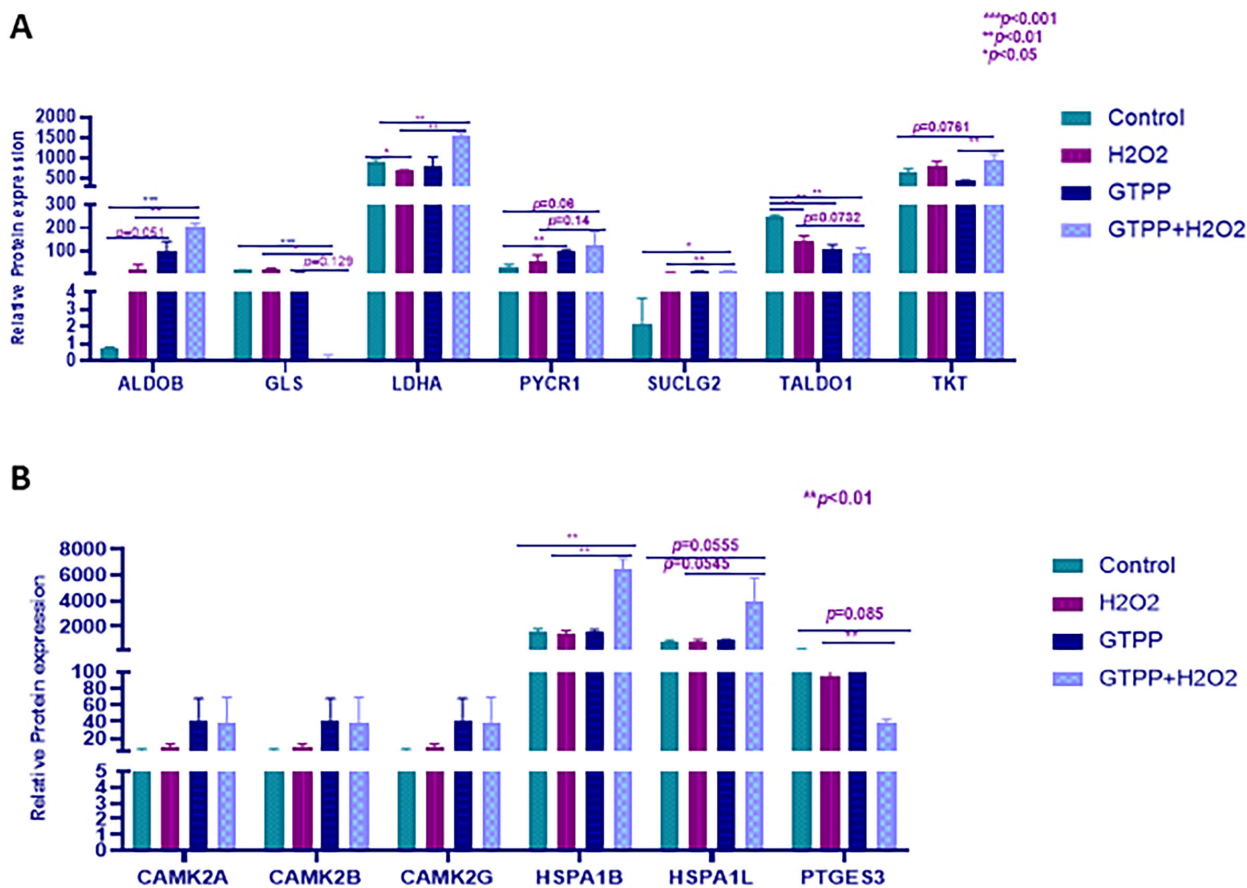


Fig. 5. TRAP1 inhibition and oxidative stress induced metabolic reprogramming in colon cancer cells and activation of the heat shock response. TRAP1 inhibition under oxidative stress altered the expression of proteins regulating cellular metabolism (A) and altered the expression of proteins regulating heat shock response pathway (B).

The protein ratios between different treatment groups were calculated using the limma package and are presented in Fig. 3A–C as volcano plots. The differential proteins in each treatment group compared to the control were visualized as a bar graph separating up- and down-regulated proteins (Fig. 3D). The inhibition of TRAP1 with GTPP appeared to substantially disrupt the proteome of HCT116 cancer cells, resulting in the highest number of differentially expressed proteins. These data demonstrate that GTPP is the major driver of protein expression changes in cells after treatment.

3.3 Enrichment Analysis of Differentially Expressed Proteins

To gain insight into the role of TRAP1 in colon cancer under oxidative stress, we performed enrichment analysis of the differentially expressed proteins using Metascape [38]. The top 20 most enriched clusters for the three treatment groups are presented in Fig. 4A–C. Exposure to H₂O₂ (oxidative stress condition) induced clusters related to response to oxidative stress, transcription, nucleo-cytoplasmic transport, and metabolism of small

molecules (Fig. 4A). Two of these enrichment clusters, neutrophil degranulation and cellular response to stress, were shared by all three treatments, including H₂O₂ alone, GTPP alone or GTPP+H₂O₂ (Fig. 4D). Cells exposed to GTPP alone displayed an enrichment of pathways related to RNA metabolism, endocytosis, proteolysis, and metabolic reprogramming of colon cancer (Fig. 4B). Metabolic reprogramming of colon cancer was also an enriched cluster in cells treated with the combination of GTPP and H₂O₂ (Fig. 4C). In addition, cells treated with GTPP+H₂O₂ also displayed enrichment of the heat shock factor 1 (HSF1) pathway (Fig. 4D). The HSF1 gene plays an important role in several cellular processes important for cancer development. It has been reported that HSF1 expression is associated with sporadic colon cancer [41]. The enrichment analysis of the differential proteins suggests that TRAP1 inhibition under oxidative stress alters the protein expression in cellular metabolism and heat-shock response pathways, prompting us to further investigate these two pathways.

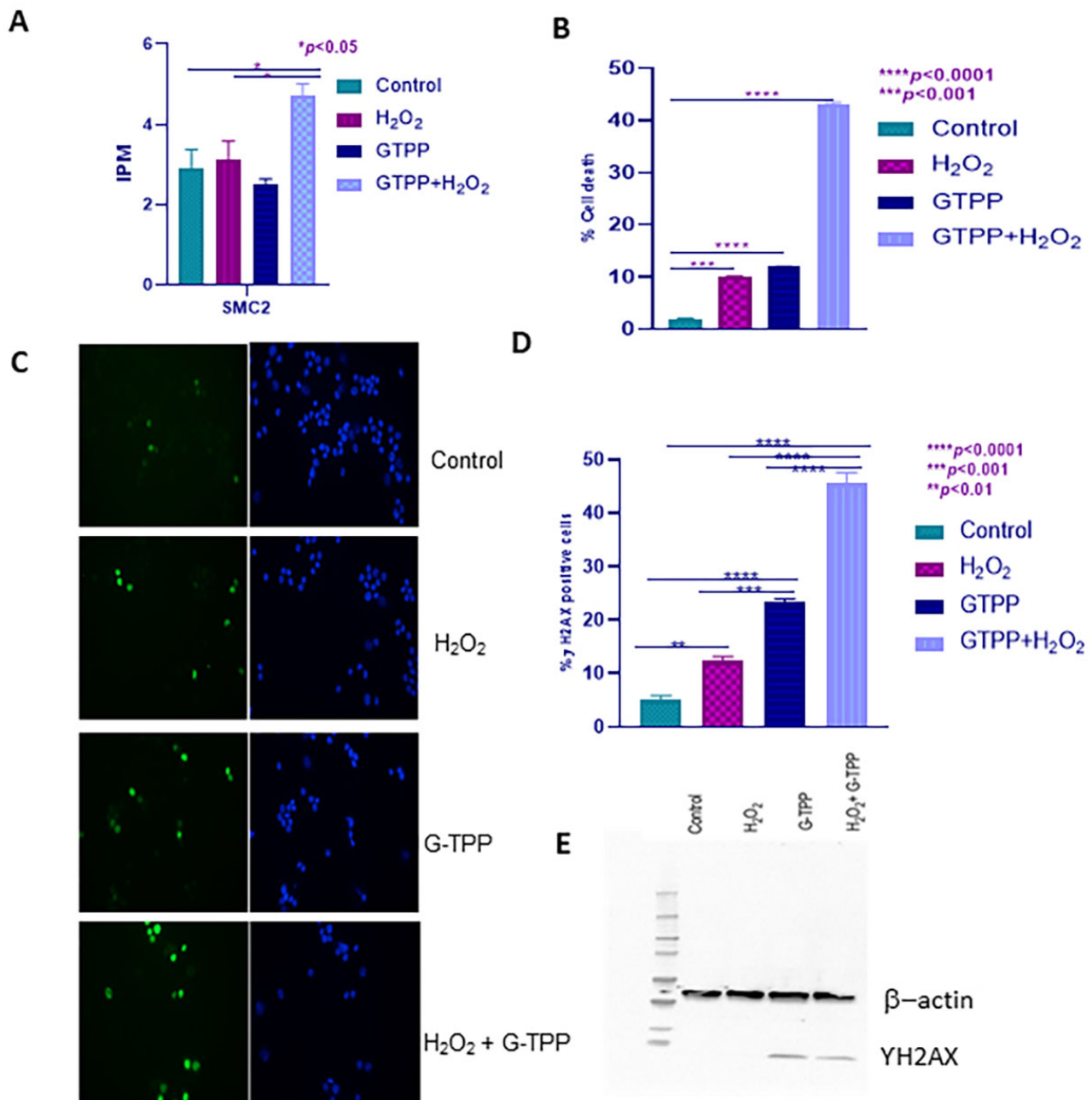


Fig. 6. TRAP1 inhibition induces cell death and DNA damage under oxidative stress. (A) SMC2 expression was significantly increased in HCT116 cells treated with GTPP+H₂O₂ compared to control, or cells treated with 10 μ M H₂O₂ alone ($p < 0.05$). (B) TRAP1 inhibition under oxidative stress in colon cancer cells increases the cell death by more than 4-fold. Treatment with the combination of GTPP+H₂O₂ induced significantly more cell death compared to treatment with H₂O₂ ($p < 0.001$) or GTPP ($p < 0.001$) alone. (C) γ H2AX expression in HCT116 cells was examined after 24 hours of treatment. Representative images are of nuclear stain in blue (DAPI) and γ H2AX in green are shown. (D) Percent positive γ H2AX were compared across using one way ANOVA followed by Tukey post hoc analysis. (E) Western-blot confirmed the expression of γ H2AX following the treatment with TRAP1 inhibitor under oxidative conditions.

3.4 TRAP1 Inhibition Under Oxidative Stress Enhances the Shift to Aerobic Glycolysis in Colon Cancer Cells

Previous reports examining the role of TRAP1 in cancer have indicated a role of TRAP1 in the induction of aero-

bic glycolysis [42,43]. Our proteomic data also showed an enrichment of metabolic reprogramming in the colon cancer pathway. To enable further inquiry into the direction of the shift in metabolism, we examined the protein expression of

genes regulating cellular energetics identified by the enrichment analysis. The shift from oxidative phosphorylation to aerobic glycolysis was evident based on the induction of glycolytic genes in the cells undergoing TRAP1 inhibition (Fig. 5A). Fructose-bisphosphate aldolase B (ALDOB) catalyzes the hydrolysis of fructose 1,6 biphosphate (FBP) to glyceraldehyde 3 phosphate and dihydroxyacetone in glycolysis. Our study showed a significant increase in the expression of ALDOB in the cells treated with GTPP+H₂O₂ compared to the control ($p < 0.001$) and cells treated with H₂O₂ alone ($p < 0.01$) (Fig. 5A). Glutaminase 1 (GLS1) is a glutamine metabolism enzyme that catalyzes the conversion of glutamine to glutamate [44]. TRAP1 inhibition under oxidative stress conditions resulted in repression of GLS1 expression (Fig. 5A). HCT116 cells treated with GTPP+H₂O₂ showed a significantly stronger repression of GLS1 expression ($p < 0.001$) relative to the control and the cells treated with H₂O₂ alone ($p < 0.05$). Lactate dehydrogenase (LDHA) is a critical glycolytic enzyme that catalyzes the conversion of pyruvate to lactate, while reduced nicotinamide adenine dinucleotide (NADH) is oxidized to nicotinamide adenine dinucleotide (NAD). We observed significantly higher expression of LDHA in cells with TRAP1 inhibition under oxidative stress (Fig. 5A). LDHA expression was significantly induced in cells treated with GTPP+H₂O₂ compared to the cells treated with H₂O₂ ($p < 0.01$) or control ($p < 0.01$) (Fig. 5A), indicating a shift to glycolytic conditions in TRAP1-inhibited cells under oxidative stress. Pyrroline-5- carboxylate reductase 1 (PYCR1) catalyzes the conversion of pyrroline-5-carboxylate to proline while oxidizing NADH to NAD [45]. It enhances the TCA cycle under hypoxic conditions [45]. PYCR1 expression upon TRAP1 inhibition under oxidative stress is also indicative of an enhanced shift to glycolysis. Our data show that TRAP1 inhibition with ($p = 0.06$) and without ($p < 0.01$) oxidative stress induces PYCR1 expression when compared to untreated cells (Fig. 5A). The *SUCLG2* gene encodes succinate dehydrogenase (SDH). This enzyme catalyzes the conversion of succinate to fumarate. Under inflammatory stress, the SDH enzyme has been shown to drive the metabolic shift from oxidative phosphorylation to aerobic glycolysis [46]. Our data showed a significant induction of *SUCLG2* expression under TRAP1-inhibited conditions relative to the untreated cells both with ($p < 0.05$) and without oxidative stress ($p < 0.01$) (Fig. 5A). Transaldolase 1 (TALDO1) is an enzyme in the pentose phosphate pathway that catalyzes the conversion of sedheptulose-7-phosphate (S7P) and GAP into erythrose-4-phosphate and fructose 6 phosphate [47,48]. The repression of TALDO1 under TRAP1 inhibition was observed both with ($p < 0.01$) and without oxidative stress ($p < 0.01$). Transketolase (TKT) is an enzyme in the pentose phosphate pathway (PPP) [49]. Its activity enables the generation of sugar phosphates for glycolysis [49]. We observed an increase in TKT expression

under oxidative stress in TRAP1-inhibited cells ($p < 0.01$). Together, these results suggest that inhibition of TRAP1 under oxidative stress conditions induces a shift to aerobic glycolysis in colon cancer cells.

3.5 TRAP1 Inhibition Under Oxidative Stress Induces the Heat Shock Transcription Factor (HSF1) Response

HSF1 is a transcription factor conventionally known to respond to cellular stress [50] and is central to NAD⁺ metabolism [51]. Our data showed an enrichment of proteins in the HSF1 transactivation pathway (Fig. 4D) with TRAP1 inhibition and oxidative stress. Calcium/calmodulin-dependent protein kinase 2 (CAMK2) is a serine threonine kinase reported to increase the phosphorylation and transactivation of HSF1 [52]. The CAMK2 proteins CAMK2A, CAMK2B and CAMK2G showed an increasing trend after treatment with GTPP with and without oxidative stress (Fig. 5B). HSPA1B is a heat shock response protein belonging to the HSP70 family of chaperone proteins associated with poor prognosis in colon cancer [53]. TRAP1 inhibition under oxidative stress showed a significantly higher expression of HSPA1B compared to the cells under oxidative stress alone or TRAP1 inhibition alone ($p < 0.01$) (Fig. 5B). HSPA1L is also a HSP70 family of heat shock proteins associated with poor prognosis in colon cancer [53]. TRAP1 inhibition under oxidative stress showed a trend of induction of HSPA1L protein when compared to untreated cells ($p = 0.05$). Prostaglandin E synthase 3 (PTGES3) is an oncogene overexpressed in colon cancer [54]. TRAP1 inhibition under oxidative stress significantly repressed PTGES3 expression in cells under oxidative stress ($p < 0.01$). Together, our results show alterations in several stress proteins downstream of the HSF1 transcription factor under treatment with GTPP+H₂O₂.

3.6 TRAP1 Inhibition under Oxidative Stress Induces Cell Death and DNA Damage

Induction of apoptosis after GTPP treatment due to an increase in ROS and the release of cytochrome C in colon cancer cells has been reported in several studies. Proteomic data from our study showed a significant increase in the expression of DNA damage and the apoptotic gene SMC2 (Fig. 6A). HCT116 cells treated with GTPP+H₂O₂ showed higher SMC2 expression than control cells. SMC2 expression was also significantly higher in cells treated with GTPP+H₂O₂ than in cells treated with H₂O₂ or GTPP alone. To obtain a quantitative estimate of the impact of TRAP1 inhibition under oxidative stress, cell death and DNA damage were evaluated after treatment. Cell death was increased almost 4-fold in cells treated with GTPP+H₂O₂ compared with cells treated with H₂O₂ ($p < 0.001$) or GTPP ($p < 0.001$) alone (Fig. 6B). Induction of DNA damage as indicated by double strand DNA breaks was estimated by γ H2AX staining (Fig. 6C–D) and western blotting (Fig. 6E). Our data show a significant increase

in double-strand DNA breaks after treatment with H₂O₂ or GTPP compared to control cells. Combination treatment with H₂O₂ and GTPP resulted in the highest degree of DNA damage when compared to no treatment or single treatment of H₂O₂ or GTPP alone.

4. Discussion

TRAP1 plays a critical role in regulating the cellular metabolism observed in several cancers and the resultant rise in metabolic reprogramming and oxidative stress. We divided the TCGA CRC cancer data into patients with +1/−1 SD of NFKB1 expression. We used this gene as a marker for oxidative stress. We further divided these groups of patients into low and high TRAP1 expression groups. Our results showed that a reduction in TRAP1 expression has a significant impact on survival when it co-occurs with high NFKB1 expression. Additionally, the percentage of patients developing new neoplasms after initial therapy was also significantly higher when TRAP1 expression was high in the high oxidative stress group. These results suggest that patients with high NFKB1 expression may have an improved prognosis if treated with TRAP1 inhibitors. Comparing the gene expression profiles of patients with high and low TRAP1 expression in the high oxidative stress group revealed an enrichment in pathways related to cellular metabolism, RNA splicing and cell division. These results suggest that altered TRAP1 expression and associated oxidative stress in colon cancer may be associated with significant changes in gene expression and disease outcomes for patients with colon cancer.

To gain further insight into the role of TRAP1 under oxidative stress in colon cancer, we performed a proteomic study in HCT116 cells. HCT116 cells have been reported to display an increased glycolytic phenotype relative to adjacent nontumor cells [42,43,55]. A recent report from our lab also showed a differential redox phenotype between various colon cancer cell lines after TRAP1 inhibition and a wide range of responses to G-TPP treatment through the induction of variable ER stress responses and ROS accumulation [20]. Based on the findings of our study and several previous reports, the role of TRAP1 in cancer appears to be context dependent [20,56]. A higher concentration of ROS alters the gut microenvironment to enable disease progression [7]. We treated HCT116 cells with H₂O₂ to induce oxidative stress and GTPP to inhibit TRAP1. The combination of GTPP and H₂O₂ was administered to mimic TRAP1 inhibition under oxidative stress. Assessment of the proteomic data through hierarchical clustering, PCA plots and sample tree suggested that TRAP1 inhibition was the major driver in the difference in protein expression followed by oxidative stress. This phenomenon was also reflected in the differences in gene expression. The maximum number of differentially expressed genes was discovered in HCT116 cells treated with GTPP compared to the control.

Previous research to understand the role of TRAP1 in cancer has revealed a regulatory role of TRAP1 in cellular respiration, differentiation, redox homeostasis, and oxidative stress-induced cell death. Our current study, through analysis of the cellular proteomic profiles, further identified functional enrichment of metabolic reprogramming of colon cancer and the HSF1 transactivation pathway modulated by TRAP1 under oxidative stress conditions. These results mirror and are consistent with previous reports and gene expression analysis of TCGA data on the role of TRAP1 in regulating the shift from oxidative phosphorylation to aerobic glycolysis [57–62].

Our study found a relatively low degree of DNA damage with the treatment of oxidative stress or TRAP1 inhibition alone but a significantly higher degree of DNA damage with the combination treatment of oxidative stress and TRAP1 inhibition. Not surprisingly, the induction of the cellular stress response was only evident in the cells with combination treatment, as supported by the upregulation of the DNA damage response gene SMC2 only in combination treatment. This phenotype was further validated with cell viability assays and γ H2AX staining.

5. Conclusions

Together, our results show that repression of TRAP1 under oxidative stress induces the DNA damage response, metabolic reprogramming and cellular stress response. Our findings support the therapeutic potential of TRAP1 in colon cancer with a high degree of oxidative stress.

Availability of Data and Materials

The original TCGA dataset are available on <https://www.cbioportal.org/datasets>. The other datasets used and/or analyzed during the current study are available from the corresponding author on reasonable request.

Author Contributions

Conceptualization, RC, SP. Methodology, PD, NB. Software, NB, PD. Validation, NB, PD and LS. Formal analysis, NB, PD and LS. Investigation, RC. Resources, RC and SP. Data curation, NB, PD, RC, SP and LS. Writing—original draft preparation, NB, PD. Writing—review and editing, RC, SP, NB, PD and LS. Visualization, NB, PD. Supervision, RC. Project administration, RC. Funding acquisition, RC. All authors have read and agreed to the published version of the manuscript.

Ethics Approval and Consent to Participate

Not applicable.

Acknowledgment

We thank Dr. Noah Shroyer's laboratory for the gift of the HCT116 cell line, and Dr. Hong-Yuan Tsai for technical support.

Funding

This work was supported by NIH/NCI grants R01CA211892 and R01CA276173.

Conflict of Interest

The authors declare no conflict of interest. Given her role as Guest Editor and Editorial Board Member, Ru Chen had no involvement in the peer-review of this article and has no access to information regarding its peer review. Full responsibility for the editorial process for this article was delegated to Alfonso Urbanucci.

Supplementary Material

Supplementary material associated with this article can be found, in the online version, at <https://doi.org/10.31083/j.fbl2809227>.

References

- [1] Huang D, Sun W, Zhou Y, Li P, Chen F, Chen H, *et al.* Mutations of key driver genes in colorectal cancer progression and metastasis. *Cancer and Metastasis Reviews*. 2018; 37: 173–187.
- [2] Grady WM, Markowitz S. Genomic instability and colorectal cancer. *Current Opinion in Gastroenterology*. 2000; 16: 62–67.
- [3] Grady WM, Carethers JM. Genomic and epigenetic instability in colorectal cancer pathogenesis. *Gastroenterology*. 2008; 135: 1079–1099.
- [4] Rao CV, Yamada HY. Genomic instability and colon carcinogenesis: from the perspective of genes. *Frontiers in Oncology*. 2013; 3: 130.
- [5] Pino MS, Chung DC. The chromosomal instability pathway in colon cancer. *Gastroenterology*. 2010; 138: 2059–2072.
- [6] Cooke MS, Evans MD, Dizdaroglu M, Lunec J. Oxidative DNA damage: mechanisms, mutation, and disease. *FASEB Journal*. 2003; 17: 1195–1214.
- [7] Lin S, Li Y, Zamyatnin AA, Jr, Werner J, Bazhin AV. Reactive oxygen species and colorectal cancer. *Journal of Cellular Physiology*. 2018; 233: 5119–5132.
- [8] Sorolla MA, Hidalgo I, Sorolla A, Montal R, Pallisé O, Salud A, *et al.* Microenvironmental Reactive Oxygen Species in Colorectal Cancer: Involved Processes and Therapeutic Opportunities. *Cancers*. 2021; 13: 5037.
- [9] Xie S, Wang X, Gan S, Tang X, Kang X, Zhu S. The Mitochondrial Chaperone TRAP1 as a Candidate Target of Oncotherapy. *Frontiers in Oncology*. 2021; 10: 585047.
- [10] Basak D, Uddin MN, Hancock J. The Role of Oxidative Stress and Its Counteractive Utility in Colorectal Cancer (CRC). *Cancers*. 2020; 12: 3336.
- [11] Maddalena F, Simeon V, Vita G, Bochicchio A, Possidente L, Sisinni L, *et al.* TRAP1 protein signature predicts outcome in human metastatic colorectal carcinoma. *Oncotarget*. 2017; 8: 21229–21240.
- [12] Chen R, Lai LA, Brentnall TA, Pan S. Biomarkers for colitis-associated colorectal cancer. *World Journal of Gastroenterology*. 2016; 22: 7882–7891.
- [13] Chen R, Pan S, Lai K, Lai LA, Crispin DA, Bronner MP, *et al.* Up-regulation of mitochondrial chaperone TRAP1 in ulcerative colitis associated colorectal cancer. *World Journal of Gastroenterology*. 2014; 20: 17037–17048.
- [14] Sciacovelli M, Guzzo G, Morello V, Frezza C, Zheng L, Nannini N, *et al.* The mitochondrial chaperone TRAP1 promotes neoplastic growth by inhibiting succinate dehydrogenase. *Cell Metabolism*. 2013; 17: 988–999.
- [15] May D, Pan S, Crispin DA, Lai K, Bronner MP, Hogan J, *et al.* Investigating neoplastic progression of ulcerative colitis with label-free comparative proteomics. *Journal of Proteome Research*. 2011; 10: 200–209.
- [16] Pak MG, Koh HJ, Roh MS. Clinicopathologic significance of TRAP1 expression in colorectal cancer: a large scale study of human colorectal adenocarcinoma tissues. *Diagnostic Pathology*. 2017; 12: 6.
- [17] Gao H, Xing F. A novel signature model based on mitochondrial-related genes for predicting survival of colon adenocarcinoma. *BMC Medical Informatics and Decision Making*. 2022; 22: 277.
- [18] Li J, Chen D, Shen M. Tumor Microenvironment Shapes Colorectal Cancer Progression, Metastasis, and Treatment Responses. *Frontiers in Medicine*. 2022; 9: 869010.
- [19] Wu XY, Zhu Z, Gai MH. Prognostic modelling of colorectal cancer based on oxidative stress-related genes. *Journal of Cancer Research and Clinical Oncology*. 2023; 149: 10623–10631.
- [20] Tsai HY, Bronner MP, March JK, Valentine JF, Shroyer NF, Lai LA, *et al.* Metabolic targeting of NRF2 potentiates the efficacy of the TRAP1 inhibitor G-TPP through reduction of ROS detoxification in colorectal cancer. *Cancer Letters*. 2022; 549: 215915.
- [21] Liu J, Lichtenberg T, Hoadley KA, Poisson LM, Lazar AJ, Cherniack AD, *et al.* An Integrated TCGA Pan-Cancer Clinical Data Resource to Drive High-Quality Survival Outcome Analytics. *Cell*. 2018; 173: 400–416.e11.
- [22] Gao J, Aksoy BA, Dogrusoz U, Dresdner G, Gross B, Sumer SO, *et al.* Integrative analysis of complex cancer genomics and clinical profiles using the cBioPortal. *Science Signaling*. 2013; 6: p11.
- [23] Cerami E, Gao J, Dogrusoz U, Gross BE, Sumer SO, Aksoy BA, *et al.* The cBio cancer genomics portal: an open platform for exploring multidimensional cancer genomics data. *Cancer Discovery*. 2012; 2: 401–404.
- [24] Clare SE, Gupta A, Choi M, Ranjan M, Lee O, Wang J, *et al.* Progesterone receptor blockade in human breast cancer cells decreases cell cycle progression through G2/M by repressing G2/M genes. *BMC Cancer*. 2016; 16: 326.
- [25] Schneider CA, Rasband WS, Eliceiri KW. NIH Image to ImageJ: 25 years of image analysis. *Nature Methods*. 2012; 9: 671–675.
- [26] Peng H, Pan S, Yan Y, Brand RE, Petersen GM, Chari ST, *et al.* Systemic Proteome Alterations Linked to Early Stage Pancreatic Cancer in Diabetic Patients. *Cancers*. 2020; 12: 1534.
- [27] Senavirathna L, Ma C, Chen R, Pan S. Proteomic Investigation of Glyceraldehyde-Derived Intracellular AGEs and Their Potential Influence on Pancreatic Ductal Cells. *Cells*. 2021; 10: 1005.
- [28] Eng JK, Jahan TA, Hoopmann MR. Comet: an open-source MS/MS sequence database search tool. *Proteomics*. 2013; 13: 22–24.
- [29] Deutsch EW, Mendoza L, Shteynberg D, Slagel J, Sun Z, Moritz RL. Trans-Proteomic Pipeline, a standardized data processing pipeline for large-scale reproducible proteomics informatics. *Proteomics. Clinical Applications*. 2015; 9: 745–754.
- [30] Keller A, Nesvizhskii AI, Kolker E, Aebersold R. Empirical statistical model to estimate the accuracy of peptide identifications made by MS/MS and database search. *Analytical Chemistry*. 2002; 74: 5383–5392.
- [31] MacLean B, Tomazela DM, Shulman N, Chambers M, Finney GL, Frewen B, *et al.* Skyline: an open source document editor for creating and analyzing targeted proteomics experiments. *Bioinformatics (Oxford, England)*. 2010; 26: 966–968.
- [32] Pan S, Brand RE, Lai LA, Dawson DW, Donahue TR, Kim S, *et al.* Proteome heterogeneity and malignancy detection in pancreatic cyst fluids. *Clinical and Translational Medicine*. 2021; 11: e506.
- [33] Senavirathna L, Ma C, Chen R, Pan S. Spectral Library-Based

- Single-Cell Proteomics Resolves Cellular Heterogeneity. *Cells*. 2022; 11: 2450.
- [34] Wang J, Vasaiakar S, Shi Z, Greer M, Zhang B. WebGestalt 2017: a more comprehensive, powerful, flexible and interactive gene set enrichment analysis toolkit. *Nucleic Acids Research*. 2017; 45: W130–W137.
- [35] Subramanian A, Tamayo P, Mootha VK, Mukherjee S, Ebert BL, Gillette MA, *et al.* Gene set enrichment analysis: a knowledge-based approach for interpreting genome-wide expression profiles. *Proceedings of the National Academy of Sciences of the United States of America*. 2005; 102: 15545–15550.
- [36] Ritchie ME, Phipson B, Wu D, Hu Y, Law CW, Shi W, *et al.* limma powers differential expression analyses for RNA-sequencing and microarray studies. *Nucleic Acids Research*. 2015; 43: e47.
- [37] Ge X. iDEP Web Application for RNA-Seq Data Analysis. *Methods in Molecular Biology (Clifton, N.J.)*. 2021; 2284: 417–443.
- [38] Zhou Y, Zhou B, Pache L, Chang M, Khodabakhshi AH, Tanaseichuk O, *et al.* Metascape provides a biologist-oriented resource for the analysis of systems-level datasets. *Nature Communications*. 2019; 10: 1523.
- [39] Fabregat A, Sidiropoulos K, Viteri G, Forner O, Marin-Garcia P, Arnaiz V, *et al.* Reactome pathway analysis: a high-performance in-memory approach. *BMC Bioinformatics*. 2017; 18: 142.
- [40] Sies H. Hydrogen peroxide as a central redox signaling molecule in physiological oxidative stress: Oxidative eustress. *Redox Biology*. 2017; 11: 613–619.
- [41] Cen H, Zheng S, Fang YM, Tang XP, Dong Q. Induction of HSF1 expression is associated with sporadic colorectal cancer. *World Journal of Gastroenterology*. 2004; 10: 3122–3126.
- [42] Maddalena F, Condelli V, Matassa DS, Pacelli C, Scrima R, Lettini G, *et al.* TRAP1 enhances Warburg metabolism through modulation of PFK1 expression/activity and favors resistance to EGFR inhibitors in human colorectal carcinomas. *Molecular Oncology*. 2020; 14: 3030–3047.
- [43] Matassa DS, Agliarulo I, Avolio R, Landriscina M, Esposito F. TRAP1 Regulation of Cancer Metabolism: Dual Role as Oncogene or Tumor Suppressor. *Genes*. 2018; 9: 195.
- [44] Song Z, Wei B, Lu C, Li P, Chen L. Glutaminase sustains cell survival via the regulation of glycolysis and glutaminolysis in colorectal cancer. *Oncology Letters*. 2017; 14: 3117–3123.
- [45] Westbrook RL, Bridges E, Roberts J, Escribano-Gonzalez C, Eales KL, Vettore LA, *et al.* Proline synthesis through PYCR1 is required to support cancer cell proliferation and survival in oxygen-limiting conditions. *Cell Reports*. 2022; 38: 110320.
- [46] Mills EL, Kelly B, Logan A, Costa ASH, Varma M, Bryant CE, *et al.* Succinate Dehydrogenase Supports Metabolic Repurposing of Mitochondria to Drive Inflammatory Macrophages. *Cell*. 2016; 167: 457–470.e13.
- [47] Moriyama T, Tanaka S, Nakayama Y, Fukumoto M, Tsujimura K, Yamada K, *et al.* Two isoforms of TALDO1 generated by alternative translational initiation show differential nucleocytoplasmic distribution to regulate the global metabolic network. *Scientific Reports*. 2016; 6: 34648.
- [48] Samland AK, Sprenger GA. Transaldolase: from biochemistry to human disease. *The International Journal of Biochemistry & Cell Biology*. 2009; 41: 1482–1494.
- [49] Alexander-Kaufman K, Harper C. Transketolase: observations in alcohol-related brain damage research. *The International Journal of Biochemistry & Cell Biology*. 2009; 41: 717–720.
- [50] Li J, Labbadia J, Morimoto RI. Rethinking HSF1 in Stress, Development, and Organismal Health. *Trends in Cell Biology*. 2017; 27: 895–905.
- [51] Cantó C. The heat shock factor HSF1 juggles protein quality control and metabolic regulation. *The Journal of Cell Biology*. 2017; 216: 551–553.
- [52] Holmberg CI, Hietakangas V, Mikhailov A, Rantanen JO, Kallio M, Meinander A, *et al.* Phosphorylation of serine 230 promotes inducible transcriptional activity of heat shock factor 1. *The EMBO Journal*. 2001; 20: 3800–3810.
- [53] Guan Y, Zhu X, Liang J, Wei M, Huang S, Pan X. Upregulation of HSPA1A/HSPA1B/HSPA7 and Downregulation of HSPA9 Were Related to Poor Survival in Colon Cancer. *Frontiers in Oncology*. 2021; 11: 749673.
- [54] Ayiomamitis GD, Notas G, Vasilakaki T, Tsavari A, Vederaki S, Theodosopoulos T, *et al.* Understanding the Interplay between COX-2 and hTERT in Colorectal Cancer Using a Multi-Omics Analysis. *Cancers*. 2019; 11: 1536.
- [55] Rodríguez-Enríquez S, Robledo-Cadena DX, Gallardo-Pérez JC, Pacheco-Velázquez SC, Vázquez C, Saavedra E, *et al.* Acetate Promotes a Differential Energy Metabolic Response in Human HCT 116 and COLO 205 Colon Cancer Cells Impacting Cancer Cell Growth and Invasiveness. *Frontiers in Oncology*. 2021; 11: 697408.
- [56] Lettini G, Maddalena F, Sisinni L, Condelli V, Matassa DS, Costi MP, *et al.* TRAP1: a viable therapeutic target for future cancer treatments? *Expert Opinion on Therapeutic Targets*. 2017; 21: 805–815.
- [57] Yoshida S, Tsutsumi S, Muhlebach G, Sourbier C, Lee MJ, Lee S, *et al.* Molecular chaperone TRAP1 regulates a metabolic switch between mitochondrial respiration and aerobic glycolysis. *Proceedings of the National Academy of Sciences of the United States of America*. 2013; 110: E1604–E1612.
- [58] Wengert LA, Backe SJ, Bourboulia D, Mollapour M, Woodford MR. TRAP1 Chaperones the Metabolic Switch in Cancer. *Biomolecules*. 2022; 12: 786.
- [59] Wu J, Liu Y, Cho K, Dong X, Teng L, Han D, *et al.* Downregulation of TRAP1 sensitizes glioblastoma cells to temozolomide chemotherapy through regulating metabolic reprogramming. *Neuroreport*. 2016; 27: 136–144.
- [60] Masgras I, Ciscato F, Brunati AM, Tibaldi E, Indraccolo S, Curtarello M, *et al.* Absence of Neurofibromin Induces an Oncogenic Metabolic Switch via Mitochondrial ERK-Mediated Phosphorylation of the Chaperone TRAP1. *Cell Reports*. 2017; 18: 659–672.
- [61] Joshi A, Ito T, Picard D, Neckers L. The Mitochondrial HSP90 Paralog TRAP1: Structural Dynamics, Interactome, Role in Metabolic Regulation, and Inhibitors. *Biomolecules*. 2022; 12: 880.
- [62] Joshi A, Dai L, Liu Y, Lee J, Ghahhari NM, Segala G, *et al.* The mitochondrial HSP90 paralog TRAP1 forms an OXPHOS-regulated tetramer and is involved in mitochondrial metabolic homeostasis. *BMC Biology*. 2020; 18: 10.